

# Evolution of quantum knots driven by minimal surfaces

Topological Methods in Mathematical Physics — Erice, IT, September 2-6, 2022

Simone Zuccher

University of Verona, Verona, ITALY

E-mail: `simone.zuccher@univr.it`

Web page: `http://profs.sci.univr.it/~zuccher/`

In collaboration with Renzo L. Ricca

September 3rd, 2022

# Fundamental changes in the topology, Lim & Nickels (1992)

# Head-on collision of perturbed quantum vortex rings under the GPE

# Agenda

- 1 The Gross-Pitaevskii equation (GPE) and its numerical approximation
- 2 Dynamics of some vortex defects in superfluids under the GPE
- 3 Possible evolutionary scenarios
- 4 Topological quantum hydrodynamics
- 5 Defect dynamics driven by minimal surfaces
- 6 Conclusions

# Agenda

- 1 The Gross-Pitaevskii equation (GPE) and its numerical approximation
- 2 Dynamics of some vortex defects in superfluids under the GPE
- 3 Possible evolutionary scenarios
- 4 Topological quantum hydrodynamics
- 5 Defect dynamics driven by minimal surfaces
- 6 Conclusions

# The Gross-Pitaevskii equation (GPE)

For a **weakly interacting Bose-Einstein condensate**,

$$\psi_t = \frac{i}{2} \nabla^2 \psi + \frac{i}{2} (1 - |\psi|^2) \psi. \quad (1)$$

By introducing the **Madelung transformation**  $\psi = \sqrt{\rho} e^{i\theta}$ , from which  $\rho = |\psi|^2$  and  $\mathbf{u} = \nabla \theta$ , GPE can be recast in the form of the **Navier-Stokes equations**. However, vortex defects are **strictly localized** and no threads or bridges of weaker vorticity are visible, contrary to viscous flows.

⇒ **Numerical problem**. For dark structures  $\rho \rightarrow 1$  as  $|\mathbf{x}| \rightarrow \infty$  and a spectral approach based on FFT needs a **periodic initial solution on a truncated domain**. If  $\psi_0(\mathbf{x})$  is not periodic, it **must be mirrored** with consequent higher computational effort and larger memory requirements. Because of limited computational resources, the **numerical box might be too small**.

# The Gross-Pitaevskii equation (GPE)

For a **weakly interacting Bose-Einstein condensate**,

$$\psi_t = \frac{i}{2} \nabla^2 \psi + \frac{i}{2} (1 - |\psi|^2) \psi. \quad (1)$$

By introducing the **Madelung transformation**  $\psi = \sqrt{\rho} e^{i\theta}$ , from which  $\rho = |\psi|^2$  and  $\mathbf{u} = \nabla \theta$ , GPE can be recast in the form of the **Navier-Stokes equations**. However, vortex defects are **strictly localized** and no threads or bridges of weaker vorticity are visible, contrary to viscous flows.

⇒ **Numerical problem**. For dark structures  $\rho \rightarrow 1$  as  $|\mathbf{x}| \rightarrow \infty$  and a spectral approach based on FFT needs a **periodic initial solution on a truncated domain**. If  $\psi_0(\mathbf{x})$  is not periodic, it **must be mirrored** with consequent higher computational effort and larger memory requirements. Because of limited computational resources, the **numerical box might be too small**.

# The Gross-Pitaevskii equation (GPE)

For a **weakly interacting Bose-Einstein condensate**,

$$\psi_t = \frac{i}{2} \nabla^2 \psi + \frac{i}{2} (1 - |\psi|^2) \psi. \quad (1)$$

By introducing the **Madelung transformation**  $\psi = \sqrt{\rho} e^{i\theta}$ , from which  $\rho = |\psi|^2$  and  $\mathbf{u} = \nabla \theta$ , GPE can be recast in the form of the **Navier-Stokes equations**. However, vortex defects are **strictly localized** and no threads or bridges of weaker vorticity are visible, contrary to viscous flows.

⇒ **Numerical problem**. For dark structures  $\rho \rightarrow 1$  as  $|\mathbf{x}| \rightarrow \infty$  and a spectral approach based on FFT needs a **periodic initial solution on a truncated domain**. If  $\psi_0(\mathbf{x})$  is not periodic, it **must be mirrored** with consequent higher computational effort and larger memory requirements. Because of limited computational resources, the **numerical box might be too small**.

# The Free-Boundary Time-Splitting Finite-Difference method

⇒ **Solution** proposed by Caliari & Zuccher (2021).

- We perform a **change of variable**  $\eta(\mathbf{y}, t) = \psi(\mathbf{x}, t)$ , to map  $\mathbf{x} \in \mathbb{R}^3$  into  $\mathbf{y} \in (-1, 1)^3$  and choose  $y_\ell(x_\ell) = \frac{2}{\pi} \arctan\left(\frac{x_\ell}{\alpha_\ell}\right)$ ,  $\alpha_\ell > 0$
- We discretize in space with **4th-order finite differences**, near the boundaries we use one-sided 4th-order finite differences, obtaining the GPE in the form

$$z'(t) = Az(t) + \frac{i}{2} (1 - |z(t)|^2) z(t), \quad (2)$$

where  $z(t)$  is a vector of dimension (degree of freedom)  $M = m_1 \times m_2 \times m_3$ .

- We apply the **Strang time splitting** to the system above, thus yielding a new method that we call **Free Boundary Time Splitting Finite Difference (FBTSFD)** method. We solve the linear part of (2) by an **efficient approximation of the action of the matrix exponential** at machine precision accuracy; the nonlinear part is solved exactly.

# Generation of the initial condition for the GPE

We know how to deal with a single **straight vortex** (see Caliari and Zuccher (2018)) and a single **vortex ring** (see Zuccher and Caliari (2021)).

For an **arbitrary initial condition** this is what we did.

- **Biot–Savart** integral to compute the velocity field  $\mathbf{u}(\mathbf{x})$  at each position  $\mathbf{x}$ .
- **Integrate** the equation  $\mathbf{u} = \nabla\theta$  **to get the phase**  $\theta(\mathbf{x})$ , after setting a reference value  $\theta_0$  at a certain point  $\mathbf{x}_0 \in \Omega$ .
- To **avoid vortex-line singularities**: we set  $\theta = 0$  at a point sufficiently distant from a defect line and integrate along paths that start from that point and go either towards infinity or terminate on the defect line.
- Assign **density**  $\rho(\mathbf{x})$  **according to the 4th-order Padé approximation** of the steady straight vortex. Since  $\rho = \rho(r)$ , for each grid point choose  $r$  as the minimum distance from the closest vortex centerlines.

# Agenda

- 1 The Gross-Pitaevskii equation (GPE) and its numerical approximation
- 2 Dynamics of some vortex defects in superfluids under the GPE**
- 3 Possible evolutionary scenarios
- 4 Topological quantum hydrodynamics
- 5 Defect dynamics driven by minimal surfaces
- 6 Conclusions

# Time evolution and topological cascade of the torus knot $\mathcal{T}(2,9)$

# Collision of three unlinked and mutually orthogonal rings

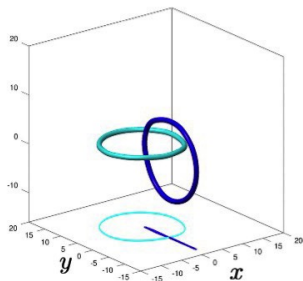
# Hopf link generated by two unlinked, unknotted elliptical defects

# Generation of a trefoil knot from two unlinked, perturbed rings

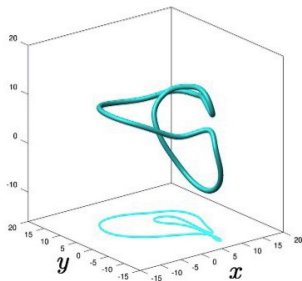
# Agenda

- 1 The Gross-Pitaevskii equation (GPE) and its numerical approximation
- 2 Dynamics of some vortex defects in superfluids under the GPE
- 3 Possible evolutionary scenarios**
- 4 Topological quantum hydrodynamics
- 5 Defect dynamics driven by minimal surfaces
- 6 Conclusions

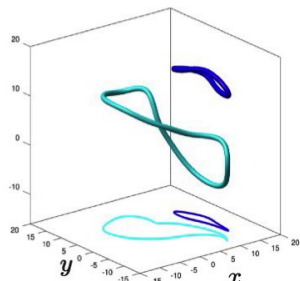
# 1. Direct topological *cascade* and collapse: Hopf link $\mathcal{T}(2, 2)$



$t = 8.80$



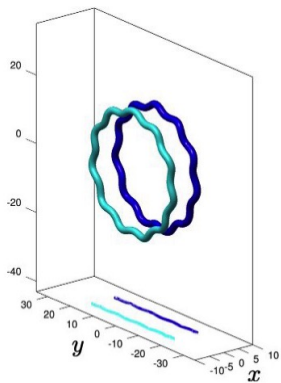
$t = 39.20$



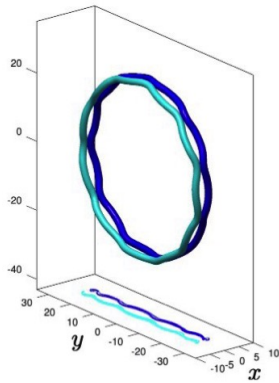
$t = 49.60$

Evolution of Hopf link  $\mathcal{T}(2, 2)$ : first reconnection to form a single unlinked, unknotted loop  $\mathcal{T}(2, 1)$  that reconnects again to form two separate small loops  $\mathcal{T}(2, 0)$ .

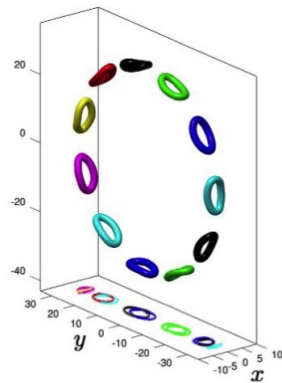
# 1. Direct topological cascade and *collapse*: HOC of perturbed rings



$t = 0.00$



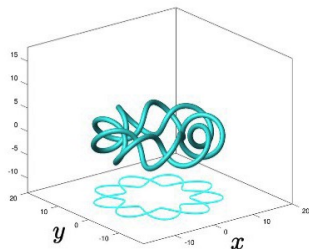
$t = 42.80$



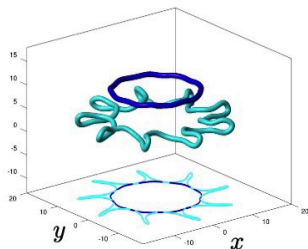
$t = 56.00$

As two perturbed vortex rings approach each other they stretch; when they are close the symmetric perturbations give rise to 11 simultaneous reconnections, equi-spaced all along the reconnection circular region; 11 small vortex rings are generated, propagating radially away from the reconnection region.

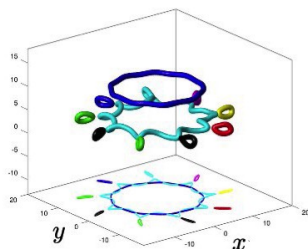
# 1. Direct topological cascade and *collapse*: torus knot $\mathcal{T}(2, 9)$



$t = 0.00$



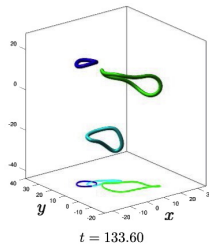
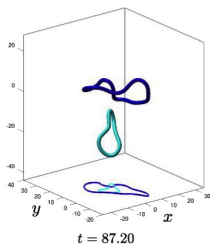
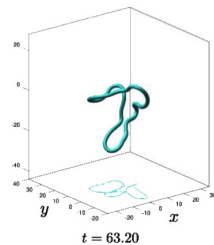
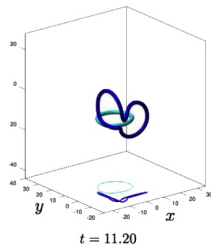
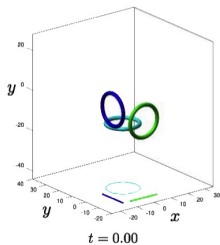
$t = 30.40$



$t = 32.80$

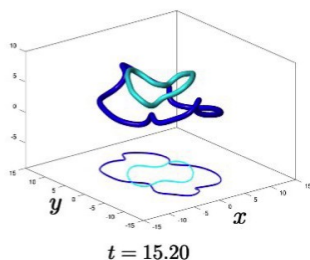
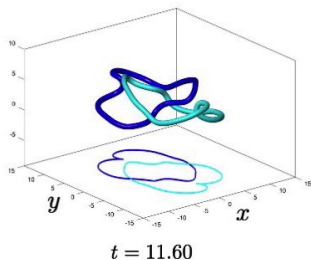
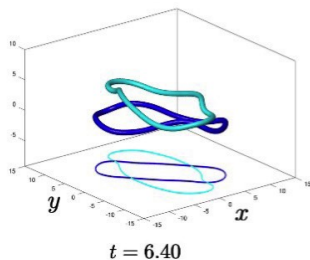
Evolution of  $\mathcal{T}(2, 9)$ : by symmetry the 9 helical coils of the knot produce 9 simultaneous reconnections. The knot type  $\mathcal{T}(2, 9)$  jumps directly to  $\mathcal{T}(2, 0)$  creating 2 separate loops: the leading ring (dark blue) and a convoluted trailing loop behind. The latter undergoes 9 simultaneous reconnections creating 9 small vortex rings. In this case the cascade process is realized by the topological collapse of a large, single structure to produce first a medium-sized, and then small-scale structures.

## 2. *Structural* and topological cycles: 3 mutually orthogonal rings



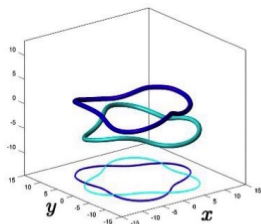
Structural cycle: 3 loops  $\rightarrow$  2 loops  $\rightarrow$  1 loop  $\rightarrow$  2 loops  $\rightarrow$  3 loops.

## 2. Structural and *topological* cycles: creation of Hopf link

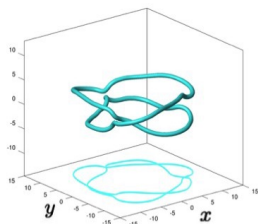


Topological cycle, generation of Hopf link with a temporary increase of topology from 2 planar ellipses: 2 unlinked loops  $\rightarrow$  Hopf link  $\mathcal{T}(2, 2) \rightarrow$  2 unlinked loops.

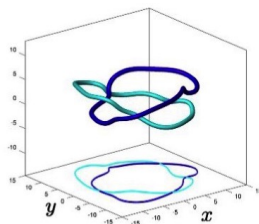
### 3. Inverse topological cascade: creation of trefoil knot



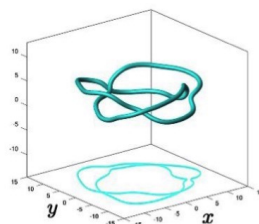
$t = 0.00$



$t = 8.80$



$t = 13.60$



$t = 17.60$

Inverse topological cascade: **evolution of topologically simple structures to produce more complex ones**. 2 initially disjoint, unknotted and unlinked perturbed rings interact to create first a single convoluted loop, then a Hopf link, and finally a trefoil knot. **First realization** of a topologically non-trivial knot starting from topologically trivial initial conditions (unknotted, unknotted loops).

2 loops  $\mathcal{T}(2, 0) \rightarrow$  1 loop  $\mathcal{T}(2, 1) \rightarrow$  Hopf link  $\mathcal{T}(2, 2) \rightarrow$  trefoil knot  $\mathcal{T}(2, 3)$

# Agenda

- 1 The Gross-Pitaevskii equation (GPE) and its numerical approximation
- 2 Dynamics of some vortex defects in superfluids under the GPE
- 3 Possible evolutionary scenarios
- 4 Topological quantum hydrodynamics**
- 5 Defect dynamics driven by minimal surfaces
- 6 Conclusions

# Topological quantum hydrodynamics

**Quantized circulation**  $\Gamma = 2\pi n$ ,  $n \in \mathbb{N}$ . **Kinetic helicity**  $\mathcal{H} = \int_{\Omega} \mathbf{u} \cdot \boldsymbol{\omega} dV$  where  $\boldsymbol{\omega} = \nabla \times \mathbf{u}$  and  $V = V(\Omega)$  is the volume of the vorticity region  $\Omega$ .

In quantum systems vorticity is singular on  $\mathcal{C}$  and the domain of vorticity has measure zero (in distributional sense) thus

$$\mathcal{H} = \Gamma \oint_{\mathcal{C}} \mathbf{u} \cdot d\mathbf{X} = \Gamma \oint_{\mathcal{C}} \nabla\theta \cdot d\mathbf{X} = 0, \quad \text{zero-helicity condition.} \quad (3)$$

If vorticity is localized on  $N$  thin filaments  $\mathcal{C}_i$  ( $i = 1, \dots, N$ )

$$\mathcal{H} = \sum_i \Gamma_i S l_i + \sum_{i \neq j} \Gamma_i \Gamma_j L k_{ij}, \quad S l_i = W r_i + T w_i, \quad (4)$$

where  $S l_i$  is the **Călugăreanu self-linking number** (topological invariant of the  $i$ -th defect), and  $L k_{ij}$  is the **Gauss linking number** (topological invariant of the link between defects  $i$  and  $j$ , with  $i \neq j, i, j = 1, \dots, N$ ).

$W r_i$  is the **writhing number** and  $T w_i$  is the **total twist**.

# Topological quantum hydrodynamics

**Quantized circulation**  $\Gamma = 2\pi n$ ,  $n \in \mathbb{N}$ . **Kinetic helicity**  $\mathcal{H} = \int_{\Omega} \mathbf{u} \cdot \boldsymbol{\omega} dV$  where  $\boldsymbol{\omega} = \nabla \times \mathbf{u}$  and  $V = V(\Omega)$  is the volume of the vorticity region  $\Omega$ .

In quantum systems vorticity is singular on  $\mathcal{C}$  and the domain of vorticity has measure zero (in distributional sense) thus

$$\mathcal{H} = \Gamma \oint_{\mathcal{C}} \mathbf{u} \cdot d\mathbf{X} = \Gamma \oint_{\mathcal{C}} \nabla\theta \cdot d\mathbf{X} = 0, \quad \text{zero-helicity condition.} \quad (3)$$

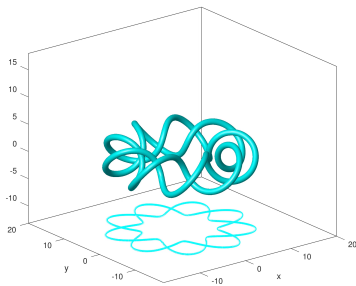
**If vorticity is localized on  $N$  thin filaments**  $\mathcal{C}_i$  ( $i = 1, \dots, N$ )

$$\mathcal{H} = \sum_i \Gamma_i S l_i + \sum_{i \neq j} \Gamma_i \Gamma_j L k_{ij}, \quad S l_i = W r_i + T w_i, \quad (4)$$

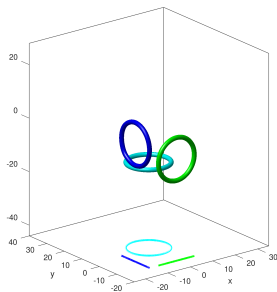
where  $S l_i$  is the **Călugăreanu self-linking number** (topological invariant of the  $i$ -th defect), and  $L k_{ij}$  is the **Gauss linking number** (topological invariant of the link between defects  $i$  and  $j$ , with  $i \neq j, i, j = 1, \dots, N$ ).

$W r_i$  is the **writhing number** and  $T w_i$  is the **total twist**.

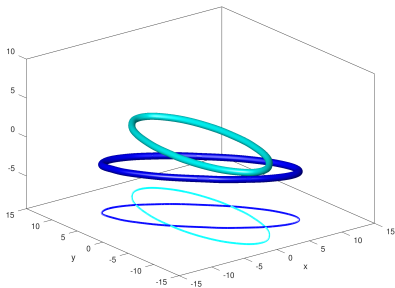
T29



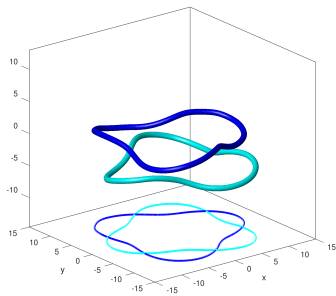
3R



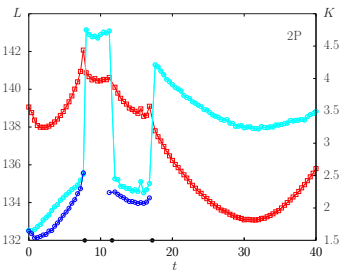
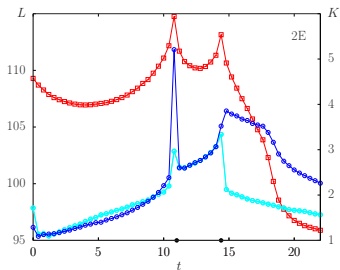
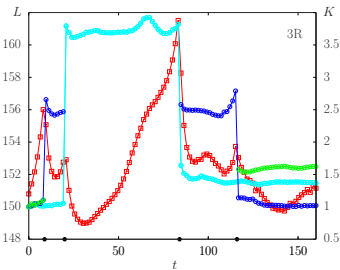
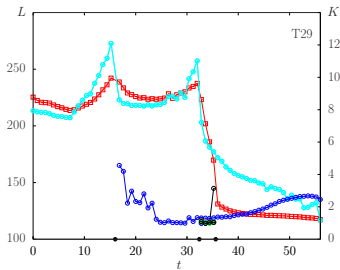
2E



2P

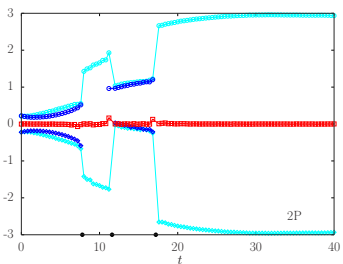
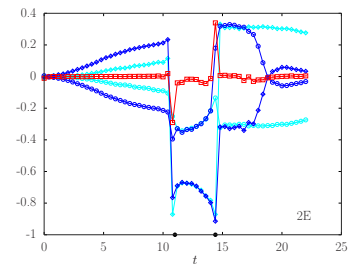
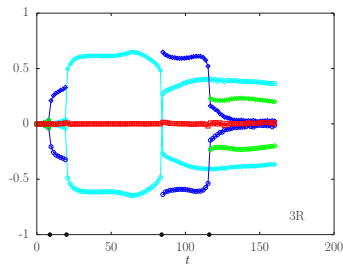
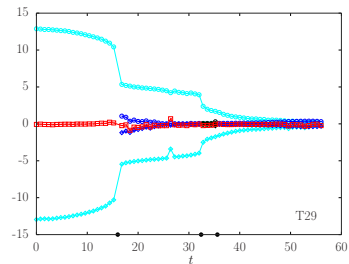


# Total length $L$ (red squares) and normalized total curvature $K$



$L$  increases as defects get closer; the **rate of change**  $|\delta L/\delta t|$  is larger after reconnections due to higher curvature of the recombined strands right after reconnection (time asymmetry and irreversibility due to **sound emission**). Pronounced **picks and drops of  $K$**  mark accurately the occurrence of **reconnection events**.

Write  $Wr$   $\circ$ , total twist  $Tw$   $\diamond$  and helicity  $\mathcal{H}$   $\square$  (red)



$\mathcal{H} \equiv 0$ , **total twist conserved** across reconnections. Apparently unbalanced jumps in 2E and 2P due to generation of Hopf link, i.e.  $|\Delta Lk_{12}| = 1$ . **Direct topological cascade** or collapse (T29): decrease in writhe, progressive decay towards unlinked, unknotted planar rings. Behavior partially reversed under **cyclic phenomena** (3R and 2E), completely reversed for **inverse cascade** (2P).

# Agenda

- 1 The Gross-Pitaevskii equation (GPE) and its numerical approximation
- 2 Dynamics of some vortex defects in superfluids under the GPE
- 3 Possible evolutionary scenarios
- 4 Topological quantum hydrodynamics
- 5 Defect dynamics driven by minimal surfaces**
- 6 Conclusions

## GPE – energy contributions

The non-dimensional form of total energy  $E_{\text{tot}}$ , **constant under GPE**, is given by

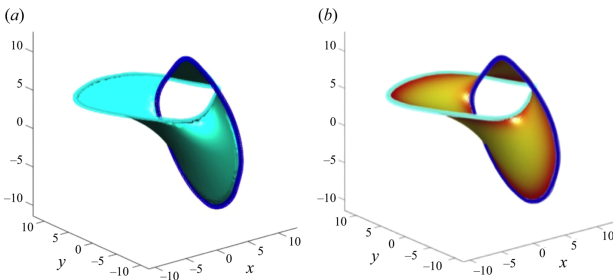
$$E_{\text{tot}} = \int \left( \frac{1}{2} |\nabla \psi|^2 - \frac{1}{2} |\psi|^2 + \frac{1}{4} |\psi|^4 \right) dV. \quad (5)$$

By Madelung's transformation  $|\nabla \psi|^2 = \rho |\nabla \theta|^2 + \frac{|\nabla \rho|^2}{4\rho} = \rho |\mathbf{u}|^2 + \frac{|\nabla \rho|^2}{4\rho}$ , hence

$$E_{\text{tot}} = \underbrace{\frac{1}{2} \int \rho |\mathbf{u}|^2 dV}_{E_k} + \underbrace{\frac{1}{8} \int \frac{|\nabla \rho|^2}{\rho} dV}_{E_q} - \underbrace{\frac{1}{2} \int \rho dV}_{E_p} + \underbrace{\frac{1}{4} \int \rho^2 dV}_{E_i}. \quad (6)$$

Density  $\rho$  reaches a constant value outside the healing region  $O(\xi)$ , but decays rapidly to zero inside the healing region, thus  $E_p$  and  $E_i$  can be taken to be constant everywhere **outside the healing regions** and **ignored**.

# Minimal surface as critical energy surface



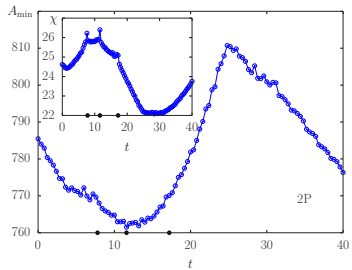
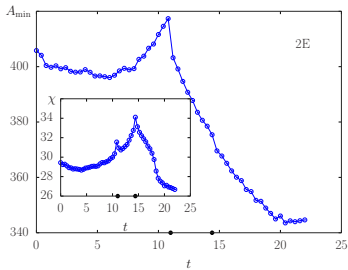
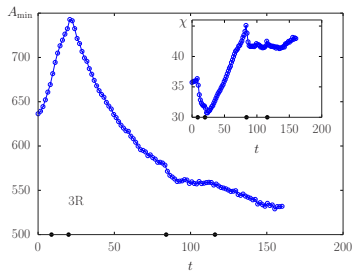
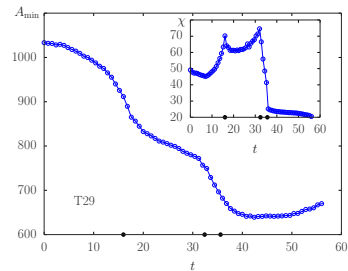
(a) Isophase surface  $S_{\min}$ ; (b) same surface color-coded by the sum  $\mathbf{e}_k + \mathbf{e}_q$

Let  $S'_{\min}$  be the portion of the minimal isophase surface  $S_{\min}$  where **density is almost constant** and compressibility is negligible.  $A(S'_{\min}) \approx A(S_{\min}) = A_{\min}$  because excluded area is small. Since  $\mathbf{u} = \nabla\theta$ , where  $\rho \approx \text{constant}$   $\nabla \cdot \mathbf{u} = 0 \Rightarrow \nabla^2\theta = 0 \forall \mathbf{x} \in S'_{\min}$ .

This shows that  $S'_{\min}$  is **harmonic** and, being a conformal immersion in  $\mathbb{R}^3$ , it is critical with respect to the **Dirichlet functional**  $D(\Theta) = \frac{1}{2} \int_{S'_{\min}} |\nabla\Theta|^2 dS$ . **Minimal isophase surfaces** are thus **privileged markers** for energy because

$$D(\psi)|_{S_{\min}} = \frac{1}{2} \int_{S_{\min}} |\nabla\psi|^2 dS = \frac{1}{2} \int_{S_{\min}} \left[ \rho |\mathbf{u}|^2 + \frac{|\nabla\rho|^2}{4\rho} \right] dS = \int_{S_{\min}} (\mathbf{e}_k + \mathbf{e}_q) dS = \mathcal{E}_k + \mathcal{E}_q .$$

$A_{\min} = A(S_{\min})$  of isophase surface; insets show  $\chi = L^2/A_{\min}$



### Direct topological cascade

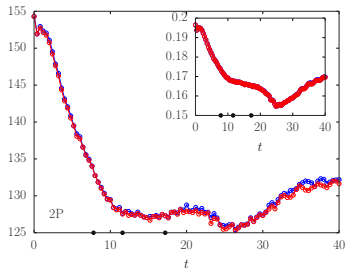
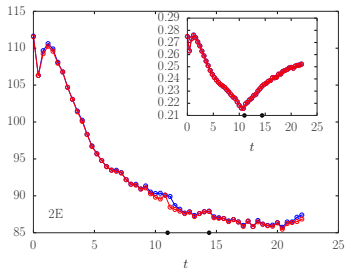
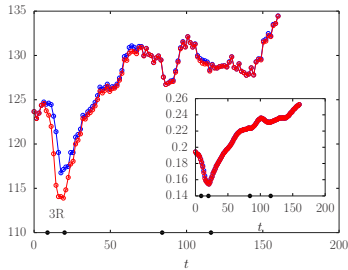
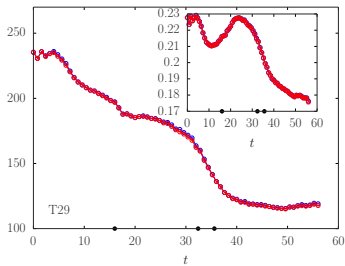
T29: monotonic decrease of  $A_{\min}$ , which increases after the formation of small rings.

**Structural cycle 3R:**  $A_{\min}$  is maximum when a single loop is present then monotonically decreases towards small rings.

**Topological cycle 2E:** same behavior. **Inverse cascade 2P:** increase of  $A_{\min}$ , peak at  $t \approx 27$ , then decrease of  $A_{\min}$ .

Evolutionary decay processes are indeed **minimal surface energy relaxation processes.**

Max[ $D(\psi)$ ] (blue) for  $\theta \in [0, 2\pi)$ , and of  $D(\psi)|_{S_{\min}}$  (red)



Plots **coincide almost everywhere** for all the cases, confirming that  $S_{\min}$  is indeed critical for energy, and proves to be an **appropriate marker for dynamics**.

Plots in **insets** show the **average values** given by Max[ $\bar{\mathcal{E}}_{kq}(S)$ ] (blue) and  $\bar{\mathcal{E}}_{kq}|_{S_{\min}}$  (red): **correlation** between **minimal surface energy relaxation** and direct topological cascade is quite evident.

# Agenda

- 1 The Gross-Pitaevskii equation (GPE) and its numerical approximation
- 2 Dynamics of some vortex defects in superfluids under the GPE
- 3 Possible evolutionary scenarios
- 4 Topological quantum hydrodynamics
- 5 Defect dynamics driven by minimal surfaces
- 6 Conclusions**

# Conclusions

- 1 Direct numerical simulations of the GPE based on a new approach that **resolves the limits** imposed by boundary conditions on a **truncated domain**.
- 2 Several test cases analyzed, **3 possible scenarios**: direct cascade and collapse, structural and topological cycles and inverse cascade.
- 3 Generation, for the first time ever, of a **trefoil knot** from the interaction of two unlinked, unknotted loops.
- 4 **Time asymmetry** of reconnections due to sound emission **confirmed** by length rate of change, see also total curvature.
- 5 **Zero Helicity Theorem confirmed**: balance between writhe, twist and linking number. Gradual nullification of writhe in decaying processes.
- 6 **Defect dynamics driven by  $S_{\min}$** ,  $\text{Max}[D(\psi)]$  corresponds to  $D(\psi)|_{S_{\min}}$ .
- 7 Direct topological cascade detected by a **monotonic decrease of  $A_{\min}$** , consistent with the observed **energy relaxation**.

## Some references

- Zuccher, S. & Ricca, R. L. 2022, Creation of quantum knots and links driven by minimal surfaces, *Journal of Fluid Mechanics*, **942**, A8.
- Caliari, M. & Zuccher, S. 2021, A fast Time Splitting Finite Difference approach to Gross-Pitaevskii equations, *Communications in Computational Physics*, **29**, 1336-1364.
- Zuccher, S. & Caliari, M. 2021, Accurate numerical determination of a self-preserving quantum vortex ring, *Journal of Physics A: Mathematical and Theoretical*, **54**, 015301.
- Caliari, M. & Zuccher, S. 2018, Reliability of the time splitting Fourier method for singular solutions in quantum fluids, *Computer Physics Communications*, **222**, 46-58.

# Questions?



$$\mathcal{H} = \sum_i \Gamma_i (Wr_i + Tw_i) + \sum_{i \neq j} \Gamma_i \Gamma_j Lk_{ij} = 0$$

**Writhing number**  $Wr_i = Wr(\mathcal{C}_i)$  is a global geometric property of a space curve  $\mathcal{C}_i$

$$Wr_i = \frac{1}{4\pi} \oint_{\mathcal{C}_i} \oint_{\mathcal{C}_i} \frac{(\mathbf{X}_i - \mathbf{X}_i^*) \cdot d\mathbf{X}_i \times d\mathbf{X}_i^*}{|\mathbf{X}_i - \mathbf{X}_i^*|^3}, \quad Wr_i \in \mathbb{R}, \quad (7)$$

where  $\mathbf{X}_i$  and  $\mathbf{X}_i^*$  denote two distinct points on  $\mathcal{C}_i$ .

**Total twist number**  $Tw_i = Tw(\mathcal{R}_i)$  is a global geometric property of a space curve  $\mathcal{C}_i$ : given the ribbon  $\mathcal{R}_i$  identified by the unit vector  $\hat{\mathbf{U}} = \hat{\mathbf{U}}(s)$ , on  $\mathcal{C}_i$

$$Tw_i = \frac{1}{2\pi} \oint_{\mathcal{C}_i} \left( \hat{\mathbf{U}} \times \frac{d\hat{\mathbf{U}}}{ds} \right) \cdot \hat{\mathbf{T}} ds \quad Tw_i \in \mathbb{R}. \quad (8)$$

Twist is independent of the particular Seifert (isophase) surface chosen.

**Linking number**  $Lk_{ij} = Lk(\mathcal{C}_i, \mathcal{C}_j)$  is a topological invariant between defects  $i$  and  $j$

$$Lk_{ij} = \frac{1}{4\pi} \oint_{\mathcal{C}_i} \oint_{\mathcal{C}_j} \frac{(\mathbf{X}_i - \mathbf{X}_j) \cdot d\mathbf{X}_i \times d\mathbf{X}_j}{|\mathbf{X}_i - \mathbf{X}_j|^3}, \quad Lk_{ij} \in \mathbb{Z}, \quad (9)$$

where  $\mathbf{X}_i \in \mathcal{C}_i$  and  $\mathbf{X}_j \in \mathcal{C}_j$ . Note that  $Wr_i = Lk_{ij}$ .

## Details on initial conditions

(1/2)

**Perturbed rings** have centerlines

$$\mathbf{X} : \begin{cases} X(t) = [R + A_i \cos(mt)] \cos t, \\ Y(t) = [R + A_i \cos(mt)] \sin t, \\ Z(t) = A_o \cos \left[ m \left( t - \frac{\pi}{6} \right) \right], \end{cases} \quad (10)$$

where  $R$  is the radius of the unperturbed ring,  $A_i$  the perturbation of the components in the  $xy$ -plane,  $A_o$  the perturbation of the out-of-plane component, and  $m$  the wavenumber.

**Torus knots**  $\mathcal{T}(p, q)$  are given by

$$\mathbf{X} : \begin{cases} X(t) = [R + r \cos(qt)] \cos(pt), \\ Y(t) = [R + r \cos(qt)] \sin(pt), \\ Z(t) = r \sin(qt), \end{cases} \quad (11)$$

where  $R$  and  $r$  are respectively the large and small radius of the torus  $\mathbb{T}$ ,  $p$  and  $q$  the number of wraps along the longitudinal and meridian (poloidal) direction of  $\mathbb{T}$ .

## Details on initial conditions

(2/2)

**HOC:** 2 rings of radius  $R = 17.4$  perturbed according to eqs. (10), with  $A_i = 0.8$ ,  $A_o = 0.22$  and wavenumber  $m = 11$ , are placed in two parallel planes  $x = \pm 4$  mirror-imaging one another.

**T29:** knot  $\mathcal{T}(2, 9)$  given by eqs. (11), with  $R = 10$ ,  $r = 3.3$ ,  $p = 2$  and  $q = 9$ , placed at the origin.

**3R:** 3 self-preserving rings with radius  $R = 8$ ; first ring centered at  $(-12, -4, 0)$  moving in the positive direction of  $x_1 (\equiv x)$ , second ring centered at  $(0, -12, -6)$  moving in the positive direction of  $x_2 (\equiv y)$ , third ring centered at  $(0.5, 4.5, -12)$  moving in the positive direction of  $x_3 (\equiv z)$ .

**2E:** 2 ellipses given in parametric form by  $(a \cos t, b \sin t)$ ; first ellipse of semi-axes  $a = 5$  and  $b = 12$  centered at the origin; second ellipse of semi-axes  $a = 4$  and  $b = 12$  centered at  $(0, 0, -3)$  and rotated by  $\pi/4$  with respect to the first.

**2P:** 2 rings of radius  $R = 10$ , perturbed according to eqs. (10) with  $A_i = 2$ ,  $A_o = 1$  and wavenumber  $m = 3$ ; first ring centered at the origin, second ring centered at  $(1, 0, -4)$  and rotated by  $\pi/3$  with respect to the first.

## Further numerical details

Case	$N_x \times N_y \times N_z$	$\alpha_1, \alpha_2, \alpha_3$	Physical domain	$\Delta t$	IC
HOPF	$171 \times 171 \times 171$	15, 15, 15	$[-821, 821]^3$	0.02	ZR
HOC	$187 \times 187 \times 187$	15, 15, 15	$[-898, 898]^3$	0.02	BS
T29	$171 \times 171 \times 171$	15, 15, 15	$[-821, 821]^3$	0.02	BS
3R	$171 \times 171 \times 171$	15, 15, 15	$[-821, 821]^3$	0.02	SP
2E	$171 \times 171 \times 171$	15, 15, 15	$[-821, 821]^3$	0.02	BS
2P	$171 \times 171 \times 171$	15, 15, 15	$[-821, 821]^3$	0.02	BS

**Table:** Case considered, degrees of freedom  $N_x \times N_y \times N_z$ ,  $\alpha_k$ -values ( $k = 1, 2, 3$ ), physical domain, time-step  $\Delta t$  and type of initial condition: ZR, rings generated as in ZR17; BS, Biot-Savart generation; SP, self-preserving rings generated by the product of initial conditions  $\psi_{0\nu}$  ( $\nu = 1, 2, 3$ ) for each of the 3 self-preserving rings.